Advances in Dynamical Systems and Applications.
ISSN 0973-5321, Volume 16, Number 2, (2021) pp. 1533-1545

https://www.ripublication.com/adsa.htm

Flow and Heat Transfer Analysis of H_2O-Al_2O_3 Nanofluid Over a Stretching Surface with Electrified Nanoparticles and Viscous Dissipation

Subhashree Panda[1], Ashok Misra[2*], Saroj Kumar Mishra[3], Aditya Kumar Pati[4] , Kamal Kumar Pradhan[5]

Centurion University of Technology and Management, Odisha, India.

*[2]*Corresponding Author: Ashok Misra*

Abstract

A steady-state flow of H_2O-Al_2O_3 nanofluid containing electrified nanoparticles over a stretchingsurface with viscous dissipation have been carried out. The boundary layer equations of the flow field in the form of coupled nonlinear partial differential equations are reduced to nonlinear ODEs using similarity transformation. The locally similar solutions of non-dimensional velocity, normalized temperature and dimensionless concentration distribution are obtained using bvp4c of MATLAB software. The numerical method is validated by comparing the results of previous investigators with the present one as a particular case by neglecting nanoparticle electrification. It is observed that the nanoparticle electrification is favorable to enhance the rate of non-dimensional mass transfer of nanoparticles and to reduce the rate of non-dimensional heat transfer of nanofluid.

Keywords. Nanoparticle Electrification, Nanofluid, Viscous dissipation

NOMENCLATURE :

Roman

C	$\rightarrow$	Concentration of the nanoparticles (Mole.m^{-3})
Cfr	$\rightarrow$	Skin friction coefficient (Pa)
D_B	$\rightarrow$	Brownian coefficient
D_T	$\rightarrow$	Thermophoresis diffusion coefficient

e	$\rightarrow$	Charge per particle (C)
E	$\rightarrow$	Electric field (Nm)
Ec	$\rightarrow$	Eckert number
k_{nf}	$\rightarrow$	Thermal conductivity of particle phase (Wm/K)
M	$\rightarrow$	Non-dimensional Electrification Parameter
Nb	$\rightarrow$	Dimensionless Brownian Motion Parameter
Nc	$\rightarrow$	Dimensionless Concentration Ratio
N_F	$\rightarrow$	Dimensionless Momentum Transfer Number
N_{Re}	$\rightarrow$	Dimensionless Electric Reynold's Number
Nt	$\rightarrow$	Dimensionless Thermophoresis Parameter
Nur	$\rightarrow$	Dimensionless Nusselt number
Pr	$\rightarrow$	Prandtl number
q_w	$\rightarrow$	Surface heat flux (W/m^2)
Re	$\rightarrow$	Reynold's number
Shr	$\rightarrow$	Sherwood's Number
S	$\rightarrow$	Dimensionless Concentration
Sc	$\rightarrow$	Schmidt Number
T	$\rightarrow$	Temperature of fluid (K)
T_w	$\rightarrow$	Wall Temperature
T_∞	$\rightarrow$	Temperature of free steam
(u, v, w)	$\rightarrow$	Velocity components for the fluid phase in x, y and z-directions respectively(m/s)
(x, y, z)	$\rightarrow$	Space co-ordinates i.e. distance along the perpendicular to plate length(m)

Greek symbols

α	$\rightarrow$	Thermal diffusivity (m^2/S)
μ	$\rightarrow$	Dynamic Viscosity of Nanofluids (kg/(ms))

ν	$\rightarrow$	Kinematic Viscosity of Nanofluids (m^2/s)
τ_w	$\rightarrow$	Skin friction (Shear stress for clear fluid)
θ	$\rightarrow$	Dimensionless Temperature
δ	$\rightarrow$	Boundary layer thickness
ε	$\rightarrow$	Diffusion parameter
ρ_f	$\rightarrow$	Density of Nanofluids (kg/m^3)
$(\rho c)_{nf}$	$\rightarrow$	Heat capacity of nanofluids ($kg/(m.S^2)$
τ	$\rightarrow$	Ratio of heat capacity of the nanoparticle and heat capacity of the fluid
φ	$\rightarrow$	Nanoparticle volume fraction
ψ	$\rightarrow$	Stream Function
η	$\rightarrow$	Similarity Variable

Superscripts

$*$	: Non-dimensional value
'	: Derivative with respect to η

1. INTRODUCTION

Due to the global demand, many industries are trying to develop fluids with significantly higher thermal conductivities as compared to the ordinary base fluids. This is because ordinary base fluids possess very less thermal conductivity.Water, oil, and ethylene glycol etc. are some of the examples of the ordinary fluids. Choi and Eastman [1] have added nano-sized particles to the ordinary base fluids for enhancing their thermal conductivity. There are various applications of the problem of nanofluid flow over a moving plate in polymer industries, metal extrusion, hot rolling industry and copper wire industry. Bachok et al. [2] have investigated the boundary layer flow of nanofluid over a moving surface in a flowing fluid. Similarly, Ishak et al. [3] and Olanrewaju et al. [4] have studied the boundary layer flow of nanofluid over a moving surface in the presence of radiation. Buongiorno [5] has studied the non-homogeneous model of nanofluid flow focusing on Brownian diffusion and thermophoresis to enhance the thermal conductivity of nanofluid. Similarly, Kuznetsov and Nield [6] have followed Buongiorno’s model to understand the influence of natural convective nanofluid passing over a vertical plate.

The electrification effect of suspended nanoparticles has been analysed by Soo [7]. He found out its influence on the dynamics of the considered particulate system. Electrification generally caused due to collision of particles within themselves and also with the wall at low temperature. This leads to produce a drag force on the ions of the system. This drag force has significant effect on the transfer of heat and concentration of the particles in the flow system. Similarly, Pati et al. [8, 10] and Patnaik et al. [9] have shown the effect of nanoparticle electrification on the boundary layer flow of nanofluid with different flow conditions. Gebhart [11] has first investigated viscous dissipation in free convection flow of nanofluid. Mohamed et al. [12] have analyzed the effect of viscous dissipation on forced convection nanofluid flow over a moving plate. A very amount of work has been focused on to study the influence of electrification of the nano-sized particles on the boundary layer flow of a nanofluid past a stretchingsurface with viscous dissipation.

Hence in the present study, the boundary layer flow of H_2O-Al_2O_3 nanofluid passed a stretching surface with the inclusion of viscous dissipation and electrification of nanoparticles is analysed to especially show the effect of electrification of nanoparticles on various flow parameters of nanofluid as well as on the heat transfer of nanofluid and concentration distribution of nanoparticles.

2. MODELLING OF THE PROBLEM

A steady state 2D boundary layer flow of H_2O–Al_2O_3 nanofluid over a stretchingsurface is modelled. At ambient temperature of T_∞ the sheet is dipped into nanofluids. Let, T and T_w be the temp of nanofluid within the boundary layer and on the plate, respectively. The velocity of the sheet is given by: $U_w(x) = \varepsilon\, U(x)$, where U is the free stream velocity of nanofluid and ε is the stretching parameter. Let C is the concentration distribution of nanoparticles which is a function of x, y and t and C_w and C_∞ be the volume concentration of nanoparticles on the sheet and in the free stream respectively. The flow geometry is shown in Fig. 1.

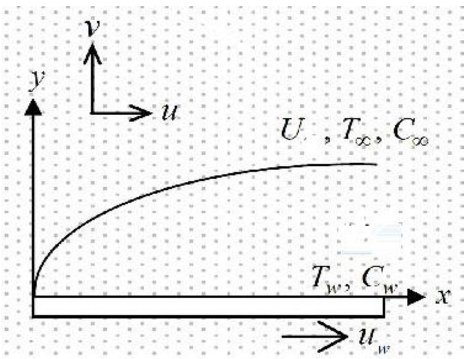

Fig. 1. Geometry of the problem

Including the phenomena of electrification of nanoparticles and viscous dissipation in the Buongiorno's model [5], the governing equations of the flow field corresponding to the above physical model are given by:

$$\frac{\partial u}{\partial x}+\frac{\partial v}{\partial y}=0 \tag{1}$$

$$u\frac{\partial C}{\partial x}+v\frac{\partial C}{\partial y}=D_B\frac{\partial^2 C}{\partial y^2}+\frac{D_T}{T}\frac{\partial^2 T}{\partial y^2}+\left(\frac{q}{m}\right)\frac{1}{F}\left(\frac{\partial(CE_X)}{\partial x}+\frac{\partial(CE_y)}{\partial y}\right) \tag{2}$$

$$\rho_{nf}\left[u\frac{\partial u}{\partial x}+v\frac{\partial u}{\partial y}\right]=-\frac{\partial p}{\partial x}+\mu_{nf}\frac{\partial^2 u}{\partial y^2}+C\rho_s\left(\frac{q}{m}\right)E_X \tag{3}$$

$$\frac{\partial p}{\partial y}=O(\delta) \tag{4}$$

$$(\rho c)_{nf}\left[u\frac{\partial T}{\partial x}+v\frac{\partial T}{\partial y}\right]=$$

$$k_{nf}\frac{\partial^2 T}{\partial y^2}+\rho_s c_s D_B\frac{\partial C}{\partial y}\frac{\partial T}{\partial y}+\frac{\rho_s c_s D_T}{T}\left(\frac{\partial T}{\partial y}\right)^2+\left(\frac{q}{m}\right)\frac{C\rho_s c_s}{F}\left(E_X\frac{\partial T}{\partial x}+E_y\frac{\partial T}{\partial y}\right)+\mu_{nf}\left(\frac{\partial u}{\partial y}\right)^2 \tag{5}$$

subjected to the boundary conditions as given below:

$$\left.\begin{array}{l} y=0, u=U_W=\varepsilon U, v=0, T=T_W, C=C_W \\ y=\infty, u=U=const, v=0, T\rightarrow T_\infty, C\rightarrow C_\infty \end{array}\right\} \tag{6}$$

The E-field can be written as:

$$\frac{\partial E_x}{\partial x}+\frac{\partial E_y}{\partial y}=\frac{\rho_s}{\varepsilon_0}\frac{q}{m} \tag{7}$$

where, ε_0 is the permittivity. Similarly, the transverse electric field is given by:

$$\frac{\partial E_y}{\partial y}=\frac{\rho_s}{\varepsilon_0}\frac{q}{m} \tag{8}$$

2.1 Similarity Transformation

Introducing the following similarity transformations [8, 9, 12]:

$$\eta=y\sqrt{\frac{U}{2\nu_f x}}, \theta=\frac{T-T_\infty}{T_W-T_\infty}, u=Uf', v=-\sqrt{\frac{\nu_f U}{2x}}\left(f-\eta f''\right), \psi=\sqrt{2\nu_f U x}f(\eta), S=\frac{C-C_\infty}{C_W-C_\infty}$$

the equation (1) is satisfied and theequations(2), (3) and (5) along with the boundary conditions (6) are converted into:

$$S''+ScfS'+\frac{Nt}{Nb}\theta''-MSc\eta S'+2Sc\frac{N_F}{N_{Re}(S+N_C+\eta S')} \tag{9}$$

$$\phi_1 f'''+ff''+2\frac{MN_b}{N_F}Sc\phi_2 S=0 \tag{10}$$

$$\frac{\phi_3\phi_4}{\Pr}\theta'' + f\theta' + \phi_3 N_b \theta' S' + \phi_3 Nt\left(\theta'\right)^2 + \left(2\frac{N_F}{N_{\mathrm{Re}}} - M\right) ScN_b\phi_3\left(S + N_c\right)\eta\theta' + \phi_5 Ec\left(f''\right)^2 = 0 \tag{11}$$

subjected to the boundary conditions,

$$\left.\begin{array}{l} \eta = 0, f(0) = 0, f'(0) = \varepsilon, \theta(0) = 1, S(0) = 1 \\ \quad \eta = \infty, f'(\infty) = 1, \theta(\infty) = 0, S(\infty) = 0 \end{array}\right\} \tag{12}$$

Considering, $\frac{T_W - T_\infty}{T_\infty} << 1$

where, $M = \left(\frac{q}{m}\right)\frac{1}{FU}E_x, N_F = \frac{U}{Fx}, \frac{1}{N_{\mathrm{Re}}} = \left(\left(\frac{q}{m}\right)^2 \frac{\rho s x^2}{U^2 \varepsilon_0}\right), N_b = \frac{\tau D_B\left(C - C_\infty\right)}{\nu_f}, Nt = \frac{\tau D_T\left(T - T_\infty\right)}{\nu_f T_\infty}$

$$\Pr = \frac{\nu_f}{\alpha_f}, Sc = \frac{\nu_f}{D_B}, N_C = \frac{C_\infty}{C_W - C_\infty}, \tau = \frac{\rho_s c_s}{\rho_f c_f}, \quad Ec = \frac{U^2}{c_f\left(T_w - T_\infty\right)}.$$

Again using the Maxwell model [13] for thermal conductivity, the thermo physical constants $\phi_1, \phi_2, \phi_3, \phi_4, \phi_5$ are obtained as:

$$\phi_1 = \frac{1}{(1 - C_\infty)^{2.5}} \frac{1}{\left[(1 - C_\infty) + C_\infty \frac{\rho_s}{\rho_f}\right]}, \phi_2 = \frac{\rho_s}{\rho_f} \frac{1}{\left[(1 - C_\infty) + C_\infty \frac{\rho_s}{\rho_f}\right]},$$

$$\phi_3 = \frac{1}{(1 - C_\infty) + C_\infty \tau}, \phi_4 = \frac{k_s + 2k_f - 2C_\infty\left(k_f - k_s\right)}{k_s + 2k_f + C_\infty\left(k_f - k_s\right)}, \phi_5 = \frac{1}{(1 - C_\infty)^{2.5}}$$

3. DISCUSSION OF RESULTS

For getting a solution of equations 9-11, these equations are converted to 1st order ordinary differential equations. Then an iterative algorithm known as Shooting technique is used to identify appropriate initial conditions $f''(0)$, $\theta'(0)$ and $S'(0)$for the resulting initial value problems (IVP) that provides the solutions to the original boundary value problems (BVP) given by equations 9-11, subjected to the boundary conditions (12). Then MATLAB bvp4c package is used to solve the BVP 9-11.

A comparative study has been carried out in Tables 1 and 2 for the validation of results. The variations of the numerical values of non-dimensional skin friction coefficient $(f''(0))$, non-dimensional rate of heat transfer$(-\theta'(0))$, non-dimensional rate of mass transfer $-S'(0)$with different values of the parameters M, N_b, N_t and E_c are presented in Table 3. Similarly, the variations of f'(η) and θ(η) of H_2O–Al_2O_3 nanofluid and dimensionless concentration distribution of nanoparticle S(η) with different values of M, N_b, N_t and E_c are depicted through the Figures 2-13. In Table 1, the present numerical values of $\frac{-\theta'(0)}{\sqrt{2}}$ have been compared with that of Mohamed et al. [12] for different P_r and are observed to be in good agreement.

Table. 1. Comparison of present values of $\frac{-\theta'(0)}{\sqrt{2}}$ with that of Mohamed et al. [12] for different P_r when N_b=N_t= E_c=M =0.

P_r	Mohamed et al.[12]	Present analysis
0.7	0.29268	0.292678
0.8	0.306917	0.306919
1.0	0.332057	0.332057
5.0	0.576689	0.576695
10.0	0.78141	0.728150

In Table 2, the computed values of $f''(0)$,$-\theta'(0)$ and$-S'(0)$in the present study have been compared with those values of Mohamed et al. [12] for different ε when N_b= N_f= N_t= E_c=0.1,S_c=10, M = 0.0,P_r=7.0 and both are observed in good agreement.

Table. 2. Comparison of present values of $f''(0)$,$-\theta'(0)$ and$-S'(0)$ withthat of Mohamed et al. [12]

Mohamed et al. [12]				Present Analysis		
ε	N_{ur}	S_{hr}	C_{fr}	N_{ur}	S_{hr}	C_{fr}
0	0.3747	1.1672	0.4696	0.37458	1.16700	0.46960
0.1	0.4705	1.3369	0.4625	0.47043	1.33674	0.46251
0.5	0.7875	1.8657	0.3288	0.78739	1.86545	0.32874
1.0	1.0717	2.3805	0	1.07170	2.38050	0
2.0	1.2994	3.3099	-1.0190	1.29904	3.30899	-1.01906

From Table 3, it is found that $f''(0)$ is enhanced with the increase of the parameters M, N_b, N_t and it is reduced with the increase of parameter E_c. It is observed that $-\theta'(0)$ shows a completely decreasing trend whereas $-S'(0)$ shows a completely increasing trend with the higher values of M, N_b, N_t and E_c.

Table. 3. Computed results of $f''(0)$, $-\theta'(0)$ and $-S'(0)$ for different values of M, Nb, Nt and Ec.

ε	E_c	φ	S_c	P_r	N_F	N_b	N_t	N_{Re}	N_c	M	$f''(0)$	$-\theta'(0)$	$-S'(0)$
0.5	0.1	0.01	1	6.2	0.1	0.1	0.1	2.0	0.1	0.0	0.31990	1.09949	-0.0594
										0.1	2.10404	0.80139	0.49057
										0.15	2.81519	0.49351	0.85612
										0.4	5.57789	-1.56941	3.303107
0.5	0.1	0.01	1	6.2	0.1	0.05	0.1	2.0	0.1	0.1	1.56565	1.05635	-0.34020
						0.1					2.10404	0.80139	0.49057
						0.2					3.08091	0.22100	0.97599
						0.5					5.59287	-1.63780	1.36483
0.5	0.1	0.01	1	6.2	0.1	0.1	0.05	2.0	0.1	0.1	1.90596	0.97524	0.50212
							0.1				2.10404	0.80139	0.49057
							0.2				2.41449	0.47374	0.93565
							0.5				2.82514	-0.22122	4.53042
0.5	0.05	0.01	1	6.2	0.1	0.1	0.1	2.0	0.1	0.1	2.12777	1.08255	0.22378
	0.1										2.10404	-0.80139	0.49057
	0.4										1.96599	-0.72067	1.93004
	0.6										1.87773	-1.58983	2.74728

1. Profiles of f'(η), θ(η) and S(η) for different values of Electrification Parameter (M):

The effect of M on f'(η), θ(η) and S(η) are shown in Figs. 2-4. Increasing parameter M has an impact in raising the profiles of f'(η) and θ(η) and in reducing the profile of S(η). These variations in the profiles of the parameters is due to the presence of Lorentz force, which acts as an accelerating force by reducing the resistance occurred due to friction. As the frictional resistance reduces the temperature of the particles also reduces.

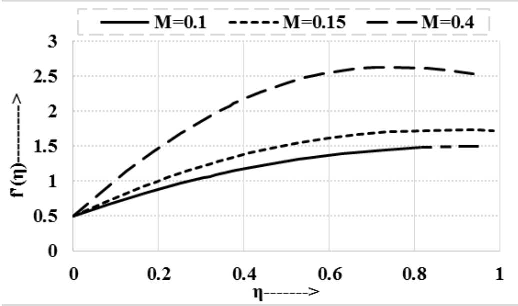

Fig. 2. Variation of $f'(\eta)$ with M

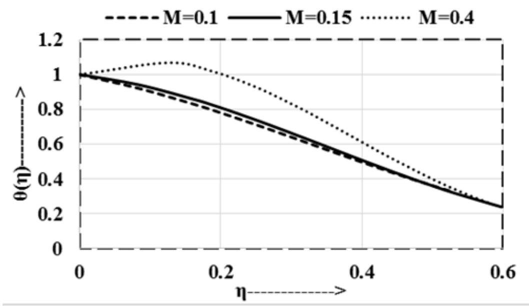

Fig. 3. Variation of $\theta(\eta)$ with *M*

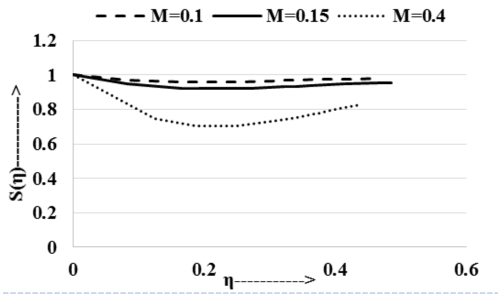

Fig. 4. Variation of *S(η)* with *M*

2. Profiles off'(η),θ(η)andS(η) for different values of diffusion parameter (N_b):

In Figs. 5-7, the effect of N_b on f'(η),θ(η) andS(η) have been depicted.Theprofilesoff'(η),θ(η) show an increasing trend, whereas S(η) shows an opposite trend with the higher values of N_b. This happens due to the effect of Brownian motion on Nb and fluid particles. The motion will be greater for small diameter particles and vice-versa. This also leads to acceleration the flow of particles.

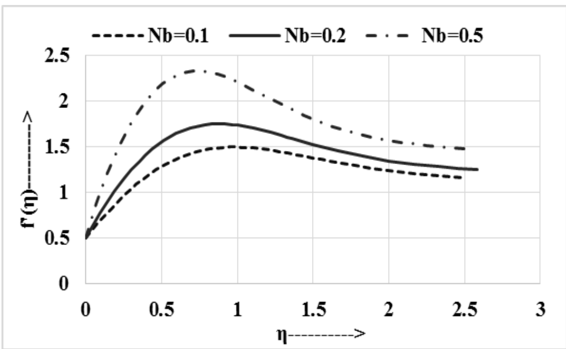

Fig. 5. Variation of $f'(\eta)$ with N_b

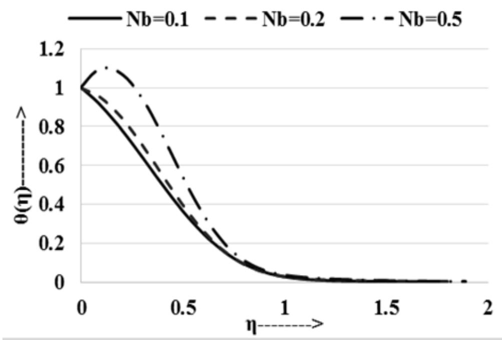

Fig. 6. Variation of $\theta(\eta)$ with N_b

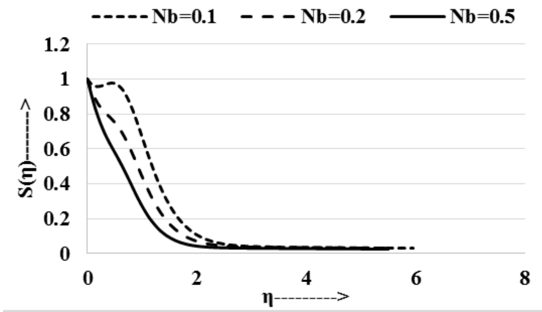

Fig. 7. Variation of *S(η)* with N_b

3. Profiles off'(η),θ(η)andS(η) for different values of Thermophoretic Parameter (N_t):

The effect of N_t on f'(η),θ(η) andS(η) are shown in Figs. 8-10. It is concluded that f'(η),θ(η) andS(η) are completely showing an increasing trend with increasing values of N_t. Thermophoresis inhibits for the reduction in temperature of the particles. The diffusion of nanoparticles in the presence of temperature gradient shows that the concentration increases with increase of Nt a little away from the plate.

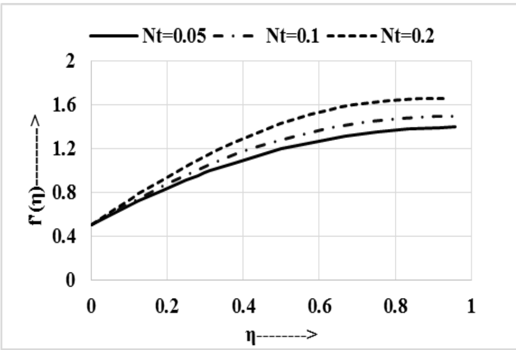

Fig. 8. Variation of $f'(\eta)$ with N_t

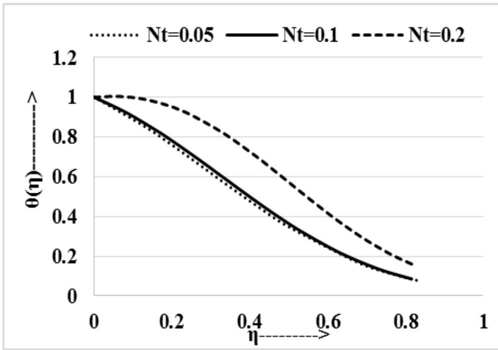

Fig. 9. Variation of θ(η) with Nt

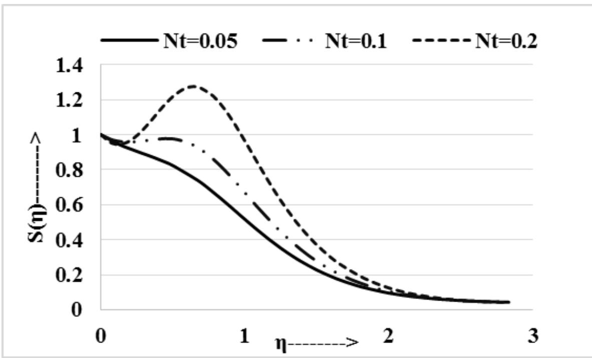

Fig. 10. Variation of *S(η)* with N_t

4. Profiles of f'(η),θ(η) and S(η) with different values of Eckert number (Ec):

Figures 11-13 show the effect of Ec on f'(η),θ(η) andS(η). Higher values of Ec cause in raising θ(η) .It is due to the fact that heat energy is stored in the fluid due to the frictional heating. But it has been observed that f'(η) and S(η) show a reverse trend for higher values of Ec.

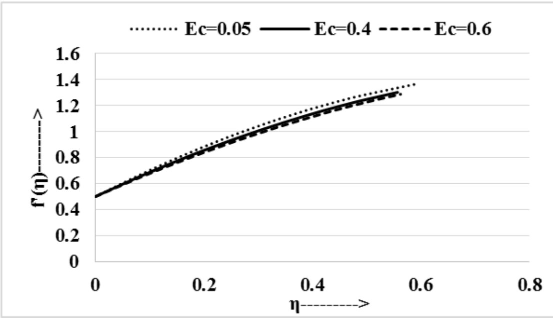

Fig. 11. Variation of $f'(\eta)$ withE_c

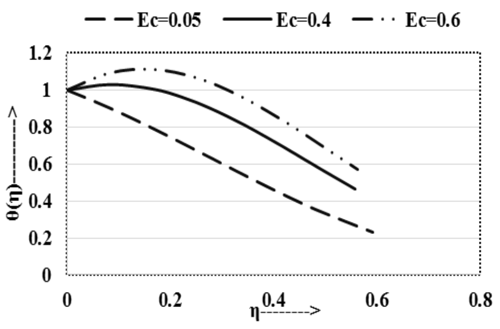

Fig. 12. Variation of $\theta(\eta)$ with E_c

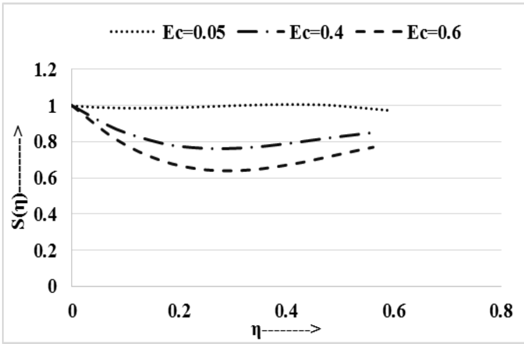

Fig. 13. Variation of *S (η)* with E_c

4. CONCLUSION

The present study deals with the effect of charged nanoparticles on the nanofluid flow over a stretching surface with viscous dissipation. The effect of various dimensional-less parameters like Diffusion parameter (N_b), electrification parameter (M), Thermophoreticparameter (N_t), Eckert number (Ec) on non-dimension velocity profile, normalized temperature profile of water-Al_2O_3 nanofluid, dimensionless concentration distribution of nanoparticles, non-dimensional skin friction coefficient, non-dimensional heat transfer of nanofluid and non-dimensional concentration distribution of nanoparticles have been analyzed through graphs and tables. The highlighted results are summarized below:

i. The higher electrification parameter M has an effect to enhance the dimensionless velocity and temperature profile of nanofluid whereas to reducenon-dimensional concentration distribution of nanoparticles.

ii. The dimensionless velocity and temperature profile shows an increasing trend, whereas the non-dimensional concentration distribution of nanoparticles show a decreasing trend with the increasing of N_b.

iii. The increasing N_t has an effect to increase dimensionless velocity and temperature of nanofluid as well as the non-dimensional concentration distribution of nanoparticles.

iv. Eckert number (E_c) plays an important role to increase the dimensionless temperature and to decrease the dimensionless velocity and concentration distribution of nanoparticles.

v. The non-dimensional skin friction coefficient is enhanced with the increase of M, N_b, N_t and it is reduced with the increase of parameter E_c. again the non-dimensional heat transfer of nanofluid shows a completely decreasing trend whereas non-dimensional concentration distribution of nanoparticles shows a completely increasing trend with the higher values of M, N_b, N_t and E_c.

REFERENCES

[1] Choi, S.U., Eastman, J. A.: Enhancing thermal conductivity of fluids with nanoparticles, Argonne National Lab., IL (United States) (1995). https://www.osti.gov/servlets/purl/196525.

[2] Bachok, N., Ishak, A. and Pop, I.: Boundary-layer flow of nanofluids over a moving surface in a flowing fluid, International Journal of Thermal Sciences, 49(9), 1663-1668 (2010). https://doi.org/10.1007/s10409-012-0014-x

[3] Ishak, A., Yacob, N.A. and Bachok, N.: Radiation effects on the thermal boundary layer flow over a moving plate with convective boundary condition, Meccanica, 46(4), 795-801 (2011).https://doi.org/10.1007/s11012-010-9338-4.

[4] Olanrewaju, P. O, Olanrewaju, M. A. and Adesanya, O.A.: Boundary layer flow of nanofluids over a moving surface in a flowing fluid in the presence of radiation, Int. J. of App. Sci. and Tech., 2(1), 1-12 (2012).

[5] Buongiorno, J.: Convective transport in nanofluids, (2006).

[6] Kuznetsov, A.V. and Nield, D.A.: Natural convective boundary-layer flow of a nanofluid past a vertical plate, International Journal of Thermal Sciences, 49(2), 243-247 (2010).

[7] Soo, S.L.: Effect of Electrification on Dynamics of a Particulate System, Industrial & Engineering Chemistry Fundamentals, 3(1), 75-80 (1964).

[8] Pati, A.K., Misra, A. and Mishra, S.K.: Heat and mass transfer analysis on natural convective boundary layer flow of a cu-water nanofluid past a vertical flat plate with electrification of nanoparticles, (2019).

[9] Pati, A.K., Misra, A. and Mishra, S.K.: Effect of electrification of nanoparticles

on heat and mass transfer in boundary layer flow of a copper water nanofluid over a stretching cylinder with viscous dissipation, (2019).

[10] Pattnaik, R., Misra, A. and Mishra, S.K.: Effect of electrification on natural convection boundary layer flow of nanofluid past a vertical plate with heat generation, JP journal of heat and mass transfer, 17, 577-595 (2019).

[11] Gebhart, B.: Effects of viscous dissipation in natural convection, Journal of fluid Mechanics, 14(2), 225-232 (1962).

[12] Mohamed, M.K.A., Noar, N.A.Z., Salleh, M.Z. and Ishak, A.: Mathematical model of boundary layer flow over a moving plate in a nanofluid with viscous dissipation, Journal of Applied Fluid Mechanics, 9(5), 2369-2377 (2016).

[13] Maxwell, J.C.: A treatise on electricity and magnetism (Vol. 1). Oxford: Clarendon Press, (1873).

[14] Roşca, N.C. and Pop, I.: Unsteady boundary layer flow of a nanofluid past a moving surface in an external uniform free stream using Buongiorno's model, Computers and Fluids, 95, 49-55 (2014).